PHYSICAL REVIEW C VOLUME 51, NUMBER 1 JANUARY 1995

Exchange process amplitudes in coherent pion production

P. A. Deutchman
Physics Department, University of Idaho, Moscow, Idaho 83843

B. Erazmus
Laboratoire de Physique Subatomique et des Technologies Associees, 2, rue de la Houssiniere, 44072 Nantes, Cedex 03, France

(Received 27 September 1994)

Calculations have been done that assess the importance of projectile-generated and target-generated pions for the exclusive reaction $^{12}C+^{12}C\rightarrow^{12}C(15.11\ MeV)+^{12}C+\pi^0$ below and near threshold. Both the amplitude for Δ formation in the target with subsequent decay to π^0's while simultaneously exciting the projectile to the $M1$ giant resonant state at 15.11 MeV, and the exchange process amplitude, in which the target and projectile exchange roles, are included in the calculations for the pion triple differential cross sections. For the first time, results of the pion energy and pion angular and ejectile angular distributions are shown with both amplitudes properly included. Also for the first time in this work, pion and ejectile distributions are shown in the laboratory frame after the appropriate relativistic transformations are performed. The projectile-generated pion amplitude is the major contributor to the pion energy and ejectile angular distribution; whereas, both amplitudes are equally important in the pion angular distribution and give rise to a unique signature for coherent pion production as seen in the c.m. frame.

PACS number(s): 25.70.−z, 24.10.Cn, 24.30.Cz

The search for coherent pion production still remains a fascinating problem. A preliminary measurement of π^0's in the reaction $^{12}C+^{12}C$ at 95 MeV/nucleon suggests the existence of a coherent subthreshold process [1]. Even if the predicted signatures of such a process are clear, its experimental identification is not easy, namely because of very small cross sections. A more detailed and more exclusive experiment is being planned. This implies low thresholds, good accuracy, and large solid angles for the detection of the reaction products. A large-solid-angle detector of photons is particularly well suited for the simultaneous registration of the gamma-ray photons coming from the π^0 and the 15.11 MeV photon coming from the nuclear excited state, along with a magnetic spectrometer detecting the ^{12}C ejectile. In order to be complete, the measurement should include the identification of both the projectile and the target nuclei.

In preparation for these experiments, sample calculations have been done to assess the importance of the amplitudes for Δ production either in the target or in the projectile. The formal solutions of the microscopic calculation for coherent Δ-hole production in equal-mass, nuclear-nuclear collisions around the pion threshold have been previously described [2–4], and we will only highlight the important factors in this Rapid Communication. The word *coherence*, as used here, refers to the *constructive interference* in the sum of Δ-hole and particle-hole terms that describe the excited-state, nuclear form factors [4]. Briefly, the second-order amplitude in the Born approximation is solved where Δ-hole states are excited in one nucleus and ordinary particle-hole states are excited in the other nucleus. The virtual Δ excitations are mitigated by π- and ρ-exchange transition interactions [5] to produce spin-isospin giant resonances. The Δ nucleon resonates through an energy-dependent width and then decays to a nucleon and pion through a decay amplitude as previously described [2]. Particle-hole and Δ-hole coefficients that weigh the various components in the nuclear excited states have been analytically solved [4] using a generalized model operator describing the spin-isospin giant resonances under the assumptions of the degenerate, schematic model [6,7]. Distortion and absorption effects have yet to be included as discussed previously [4] although an estimate of pion absorption has been made. However, at this stage, the theory is useful in assessing the pion contributions coming from the target and from the projectile and new results will be shown for the pion energy distributions as well as for the pion angular and ejectile angular distributions. Details of the present calculation along with a discussion of how the three-body kinematics and other energy dependencies effect the calculation will be presented in a subsequent paper.

If it is assumed that Δ-hole states are formed in the *target* and ordinary particle-hole states are formed in the *projectile*, and that the Δ decays from the *target*, then the amplitude for this process is given by

$$A^{P*}_{T(\Delta)\rightarrow T\pi}=\sum_{J_T M_T} A^{M_T M_P}_{J_T M_P}(\mathbf{K}_P)A^{M_T}_{J_T}(\mathbf{k}_\pi), \tag{1}$$

where $A^{M_T M_P}_{J_T M_P}(\mathbf{K}_P)$ is the amplitude for the simultaneous formation of both the projectile into a spin-isospin giant resonance of angular momentum (J_P,M_P) and the target into an intermediate nuclear state of angular momentum (J_T,M_T) which is composed of Δ-hole components. The decay of the $\Delta\rightarrow n\pi$ is described by the decay amplitude $A^{M_T}_{J_T}(\mathbf{k}_\pi)$ from the intermediate target state back to its ground state emitting a pion of momentum $\hbar\mathbf{k}_\pi$. Because the target goes back to its ground state, the pion carries away the angular momentum (J_T,M_T) in a spatial angular momentum pattern as described by Eq. (20) in Ref. [2]. Because of the Born approximation, the formation amplitude is a function of the *projectile momentum transfer* $\hbar\mathbf{K}_P=\hbar\mathbf{k}_{P_O}-\hbar\mathbf{k}_{P_F}$ where

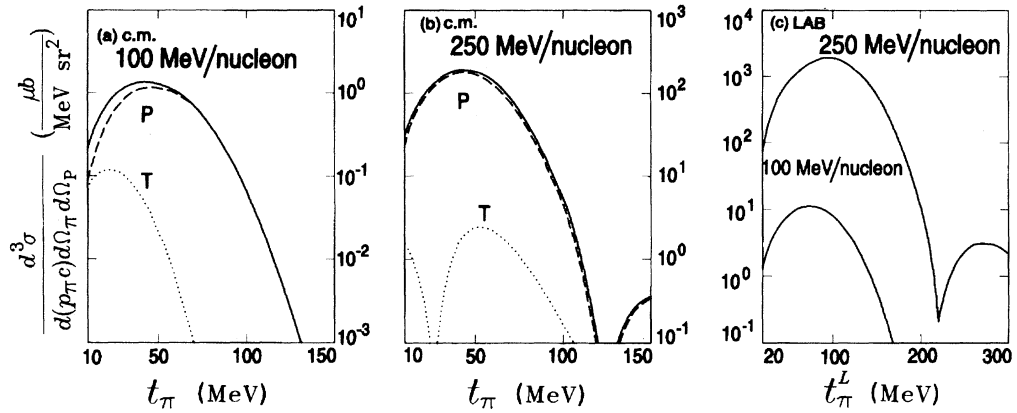

FIG. 1. (a) Triple differential cross sections in the reaction $^{12}C+^{12}C\rightarrow^{12}C$ (15.11 MeV)$+^{12}C+\pi^0$ as a function of the pion kinetic energy. The incident projectile energy in the laboratory is 100 MeV/nucleon. All other quantities are in the c.m. frame. The dashed line is the cross section for the projectile-generated pions only and the dotted line is for the target-generated pions only. The full line is the total result. (b) Triple differential cross section in the c.m. frame at 250 MeV/nucleon. (c) Triple differential cross section in the laboratory frame at 100 and 250 MeV/nucleon. All curves are calculated with the pions and ejectile in the forward direction in both frames.

$\hbar\mathbf{k}_{P_O}$ is the momentum of the initial projectile and $\hbar\mathbf{k}_{P_F}$ is the momentum of the projectile in its final state. All momenta are viewed from the nucleus-nucleus, center-of-momentum (c.m.) frame. It should be pointed out that in the detailed calculation, the formation amplitude to the *intermediate* state is a function of *intermediate* momentum transfer $\hbar\mathbf{k}_{P_O}-\hbar\mathbf{k}_P$ where $\hbar\mathbf{k}_P$ is the *intermediate* projectile momentum. Because the Δ is created in the intermediate target state, the projectile will conserve momentum from its intermediate to final projectile state or $\hbar\mathbf{k}_P=\hbar\mathbf{k}_{P_F}$. Hence, the formation amplitude is a function of projectile momentum transfer $\hbar\mathbf{K}_P$ from the initial to the final state. This will not be the case when we examine the exchange process amplitude where the Δ is formed not in the target, but in the *intermediate projectile* state. Finally, the overall amplitude in (1) is summed over the intermediate angular momentum states of the target. The projectile is left "hanging" in its giant resonant state (J_P,M_P) which for ^{12}C is the $M1$ state at 15.11 MeV. This γ decay is at low energy compared to other energies in the problem and is so slow in comparison to the nuclear target decay so that Eq. (1) is a good approximation where only the nuclear sector is considered.

Now it is assumed that the process described above is exchanged between nuclei, that is, the Δ-hole excitations and their decay with subsequent pion production all take place in the *projectile*. The *target* is then assumed to be excited to its normal giant resonant state. For simplicity in all previous calculations, it was assumed that this amplitude was identical to the amplitude in (1) giving a factor of 4 to the cross section. This turns out to be too simple and a retrace of the derivation was done for the exchange process amplitude. This results in the exchange process amplitude being given by

$$A^{T^*}_{P(\Delta)\rightarrow P\pi}=\sum_{J_PM_P} A^{M_PM_T}_{J_PM_T}(\mathbf{K}_P(\Delta))A^{M_P}_{J_P}(\mathbf{k}_\pi), \qquad (2)$$

where the roles of target and projectile are exchanged. An interesting feature occurs in the formation amplitude which is a function of the intermediate projectile momentum transfer $\hbar\mathbf{K}_P(\Delta)=\hbar\mathbf{k}_{P_O}-\hbar\mathbf{k}_P(\Delta)$ where $\hbar\mathbf{k}_P(\Delta)$ is the intermediate momentum of the projectile with the Δ formed inside. Again by subsequent momentum conservation in the Born approximation, $\hbar\mathbf{k}_P(\Delta)=\hbar\mathbf{k}_{P_F}+\hbar\mathbf{k}_\pi$ where the intermediate projectile decays into the final projectile emitting a pion. From this result, the final projectile momentum transfer becomes the vector difference $\hbar\mathbf{K}_P(\Delta)=\hbar\mathbf{K}_P-\hbar\mathbf{k}_\pi$. Hence the formation amplitude is a function of $\hbar\mathbf{K}_P-\hbar\mathbf{k}_\pi$ and not $\hbar\mathbf{K}_P$ as appears in the formation amplitude in Eq. (1). The pion takes momentum away from the projectile momentum transfer for Δ's produced inside the projectile and hence the negative sign in front of $\hbar\mathbf{k}_\pi$. Therefore, there is an asymmetry of the momentum transfers that are inputs to the formation factors depending on whether the Δ is formed in the target or in the projectile. By overall momentum conservation, $\hbar\mathbf{k}_{P_O}+\hbar\mathbf{k}_{T_O}=\hbar\mathbf{k}_{P_F}+\hbar\mathbf{k}_{T_F}+\hbar\mathbf{k}_\pi$ between initial and final states such that $\hbar\mathbf{K}_P-\hbar\mathbf{k}_\pi=-\hbar\mathbf{K}_T$, which is the negative of the target momentum transfer. In the present calculation, the formation amplitude in Eq. (2) is taken to be a function of $-\hbar\mathbf{K}_T$. The asymmetry cited above is a constant reminder of the three-body nature of our problem in the final state. Finally, the amplitudes for both processes in both nuclei are summed with the overall amplitude, including the Breit-Wigner denominator as given by Eq. (28) in Ref. [1], and the triple differential cross section as given by Eq. (17) in Ref. [13] is calculated.

The results for the pion kinetic energy distributions below and near the pion threshold are shown in Fig. 1 for the reaction $^{12}C+^{12}C\rightarrow^{12}C+^{12}C+\pi^0$ where the pion and ejectile angles are taken in the forward direction. Figures 1(a) and 1(b) show the results in the nucleus-nucleus, center-of-momentum frame, and Fig. 1(c) shows the results after relativistic transformations to the laboratory frame have been taken. The total calculation in Fig. 1(a) (full line) receives contributions from the exchange process amplitude, where the Δ is created in the projectile only (dashed line), and the target amplitude where the Δ is created in the target only (dotted line). The projectile generated pions are obtained by

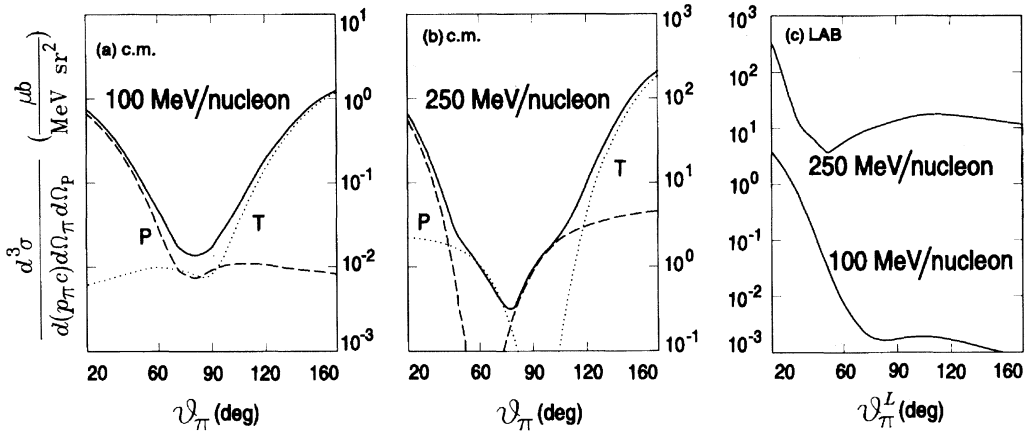

FIG. 2. (a) Pion angular distributions in the c.m. frame at 100 MeV/nucleon. (b) Pion angular distributions in the c.m. frame at 250 MeV/nucleon. The pion kinematics are fixed at $t_\pi = 60$ MeV, $\phi_\pi = 0°$ and the ejectile is fixed in the forward direction $\Theta_P = 0°$. The dashed curve is the cross section for projectile contributions only and the dotted curve is the cross section for target contributions only. The full curve is the cross section for both amplitudes contributing. (c) Pion angular distributions at the 100 and 250 MeV/nucleon with $t_\pi{}^L = 100$ MeV, $\theta_\pi{}^L = 0°$, and $\Theta_P^L = 0°$.

artificially turning off the target amplitude and visa versa for the target generated pions. As shown in Figs. 1(a) and 1(b), the main contribution to the differential cross section comes mainly from the exchange process amplitude, that is, the projectile generated pions. Figure 1(c) shows the overall pion energy distributions at 100 and 250 MeV nucleon after transformation into the laboratory frame with the pion and ejectile fixed in the forward direction.

In Fig. 2, the pion angular distributions are shown at the same incident energies. In Figs. 2(a) and 2(b), the pion kinetic energy is fixed at $t_\pi = 60$ MeV which is near the maxima in Figs. 1(a) and 1(b) with the pion and ejectile fixed in the forward direction. In Fig. 2(c), a laboratory angular distribution is shown where the laboratory pion kinetic energy is fixed at $t_\pi{}^L = 100$ MeV which roughly corresponds to the maximum of the 250 MeV/nucleon curve in Fig. 1(c). It must be remembered that the curves in the laboratory frame involve relativistic transformations of angles and energies such that each point on a curve in the laboratory corresponds to two values of angle and energy in the c.m. frame. The laboratory distributions were obtained by transforming the laboratory angles and energies into c.m. angles and energies, then calculating the c.m. cross section from those c.m. inputs and finally transforming the c.m. cross section back into a laboratory cross section. The main feature of Figs. 2(a) and 2(b) is the forward-backward peaking of the angular distributions as seen in the c.m. frame. This result shows the equal importance of the projectile- and target-generated pions, where the projectile amplitude contributes pions mainly in the forward angles, and the target amplitude contributes pions mainly in the backward angles. It also explains the dominance of the projectile-generated pions in Figs. 1(a) and 1(b) since the pions are measured in the forward direction. The angular distribution therefore gives a unique signature

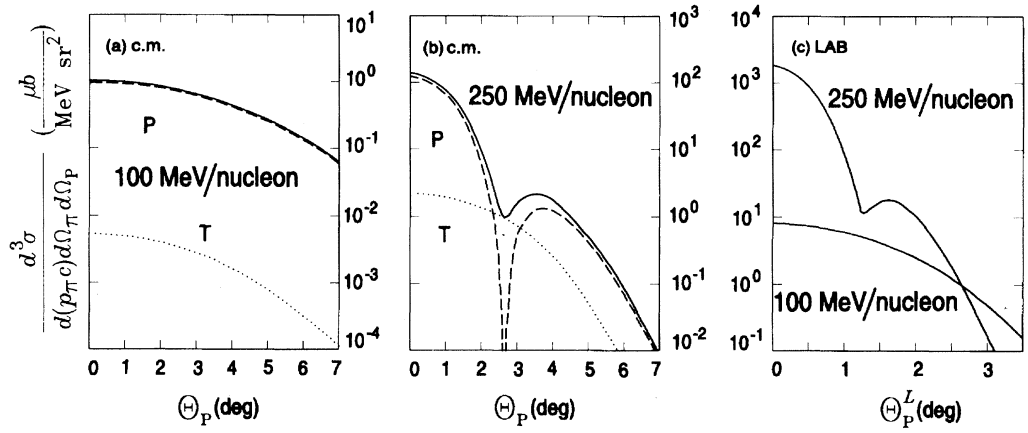

FIG. 3. (a) Ejectile angular distributions in the c.m. frame at 100 MeV/nucleon. (b) Ejectile angular distributions in the c.m. frame at 250 MeV/nucleon. The pion kinematics are fixed at $t_\pi = 60$ MeV, $\theta_\pi = 0°$ and the ejectile at $\Theta_P = 0°$. The dashed curve, dotted curve, and full curve are the same as in Figs. 2(a) and 2(b). (c) Ejectile angular distributions in the laboratory frame with $t_\pi{}^L = 100$ MeV, $\theta_\pi{}^L = 0°$, and $\Theta_P^L = 0°$.

for coherent pions coming from both nuclei. The component curves are not quite symmetric because of complicated energy dependencies of the Δ width as viewed in the nucleus-nucleus frame, and because of asymmetry terms in the phase-space, again due to the three-body nature of the final state. Angular distributions in the laboratory frame at the same incident energies where the laboratory pion kinetic energy and azimuthal angle are fixed at $t_\pi{}^L = 100$ MeV, $\phi_\pi{}^L = 0°$ and the ejectile fixed in the forward direction, $\Theta_P^L = 0°$ are shown in Fig. 2(c). The relativistic transformations give a forward angle peaking in the laboratory frame.

Finally, the ejectile angular distributions at 100 and 250 MeV/nucleon incident energy are shown in Fig. 3. Here, the main contributions come from the projectile because the pions are measured in the forward direction. The higher incident energy shows more forward peaking than the lower incident energy, indicating that the faster incident projectile "skims" by the target and is scattered less than the slower projectile. However, both results show the essential peripheral nature of these nuclear collisions.

In conclusion, these calculations show the importance of the exchange process amplitude for projectile-generated pions as well as the target-generated pion amplitude. Both amplitudes need to be included in a calculation of the pion angular distribution because they give rise to a unique signature. This may be helpful in the search for coherent pion production.

One of the authors (P.A.D.) would like to thank D. Ardouin and the Laboratoire de Physique Subatomique et des Technologies Associees for the kind hospitality and financial support during my visit to the laboratory in Nantes, France.

[1] B. Erazmus *et al.*, Phys. Rev. C **44**, 1212 (1991).
[2] P. A. Deutchman, Phys. Rev. C **45**, 357 (1992).
[3] P. A. Deutchman, Phys. Rev. C **47**, 881 (1993).
[4] P. A. Deutchman and G. Q. Li, Phys. Rev. C **47**, 2794 (1993).
[5] R. Machleidt, Adv. Nucl. Phys. **19**, 189 (1989); **19**, 354 (1989).
[6] G. E. Brown, J. A. Evans, and D. J. Thouless, Nucl. Phys. **24**, 1 (1961).
[7] J. M. Eisenberg and W. Greiner, *Microscopic Theory of the Nucleus* (North-Holland, Amsterdam, 1972), Vol. III, p. 200.